U. S. DEPARTMENT OF COMMERCE
NATIONAL OCEANIC AND ATMOSPHERIC ADMINISTRATION
NATIONAL WEATHER SERVICE
NATIONAL METEOROLOGICAL CENTER

OFFICE NOTE 307

RECENT CHANGES IN THE NEW MEDIUM-RANGE FORECAST (MRF) MODEL

PETER CAPLAN
MEDIUM-RANGE MODELING BRANCH
DEVELOPMENT DIVISION

MARCH 1985

RECENT CHANGES IN THE NEW MEDIUM-RANGE FORECAST (MRF) MODEL

On January 26, 1985, two modifications to the daily experimental runs of the new medium-range spectral model were simultaneously implemented; one was the use of "silhouette" mountains, the other a small correction of some aspects of the treatment of water vapor, to be referred to here as the virtual temperature correction. In addition to some before-and-after statistics, we will describe two cases of 120-hour forecasts in which parallel runs were made with and without modifications, so that comparisons are possible. In a run on January 9, we tested the new mountains only, while on January 24 both the mountains and the virtual temperature correction were tested.

The silhouette mountains, first described by Mintz (personal communication) and adapted at NMC by Mesinger (1985), are intended to present a more realistic profile to incident winds than can either the relatively smooth mountains in the operational spectral model or the envelope topography used at ECMWF. To generate this topography for each grid box, one first visualizes the mountains (as given by point elevations on the U.S. Navy's 1/6° topography) projected along one horizontal coordinate direction at a time. The highest elevation in each column of points is taken to represent that column. This procedure generates a composite row in each coordinate direction, and the points in these two rows are averaged to yield a representative elevation for the grid box as a whole. As can be seen from Figure 1, the mountains generated are considerably higher and richer in detail than the operational mountains. Their heights turn out to be comparable to those of the envelope mountains.

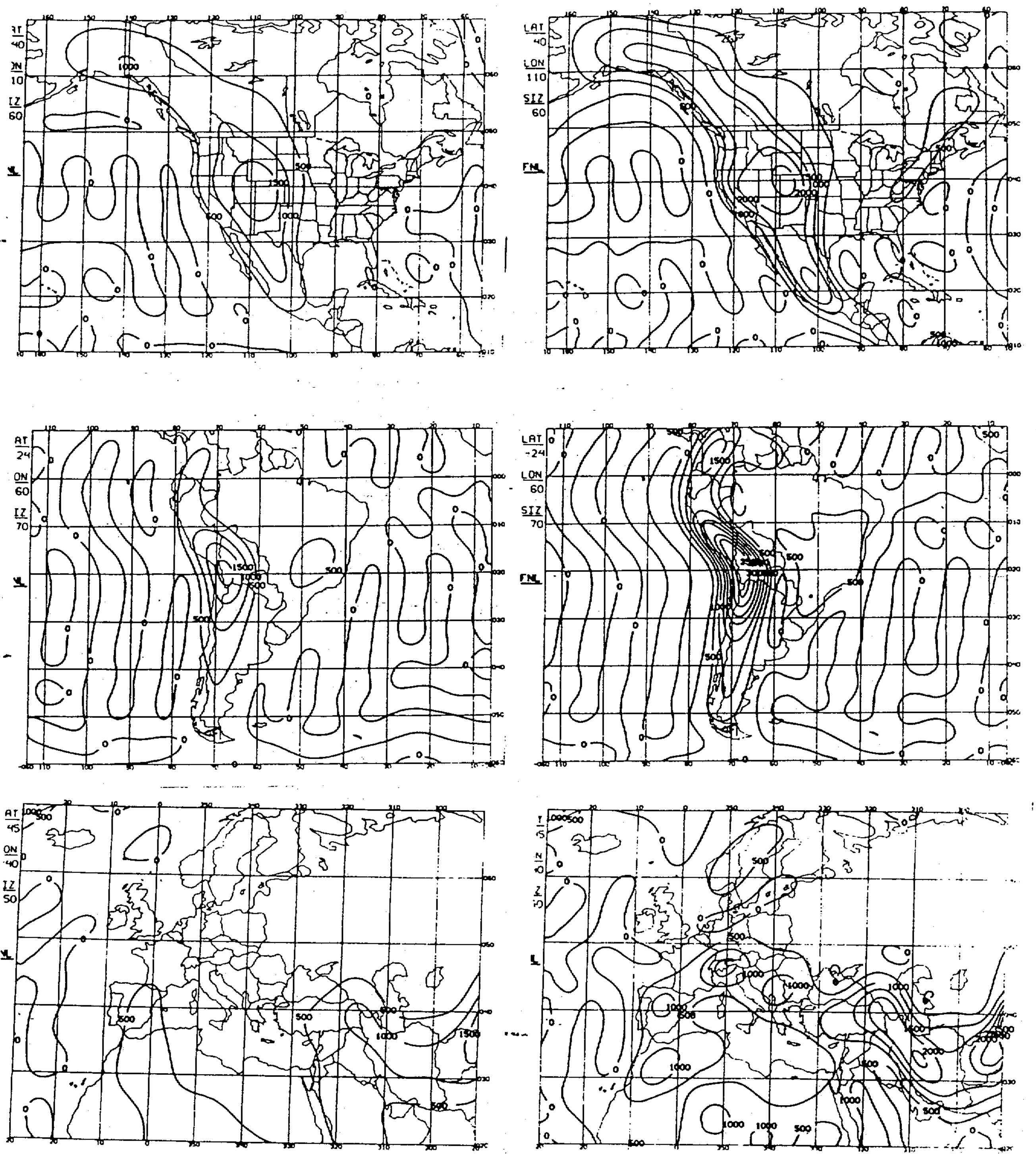

Operational | Silhouette

Figure 1. Operational topography vs. silhouette topography.

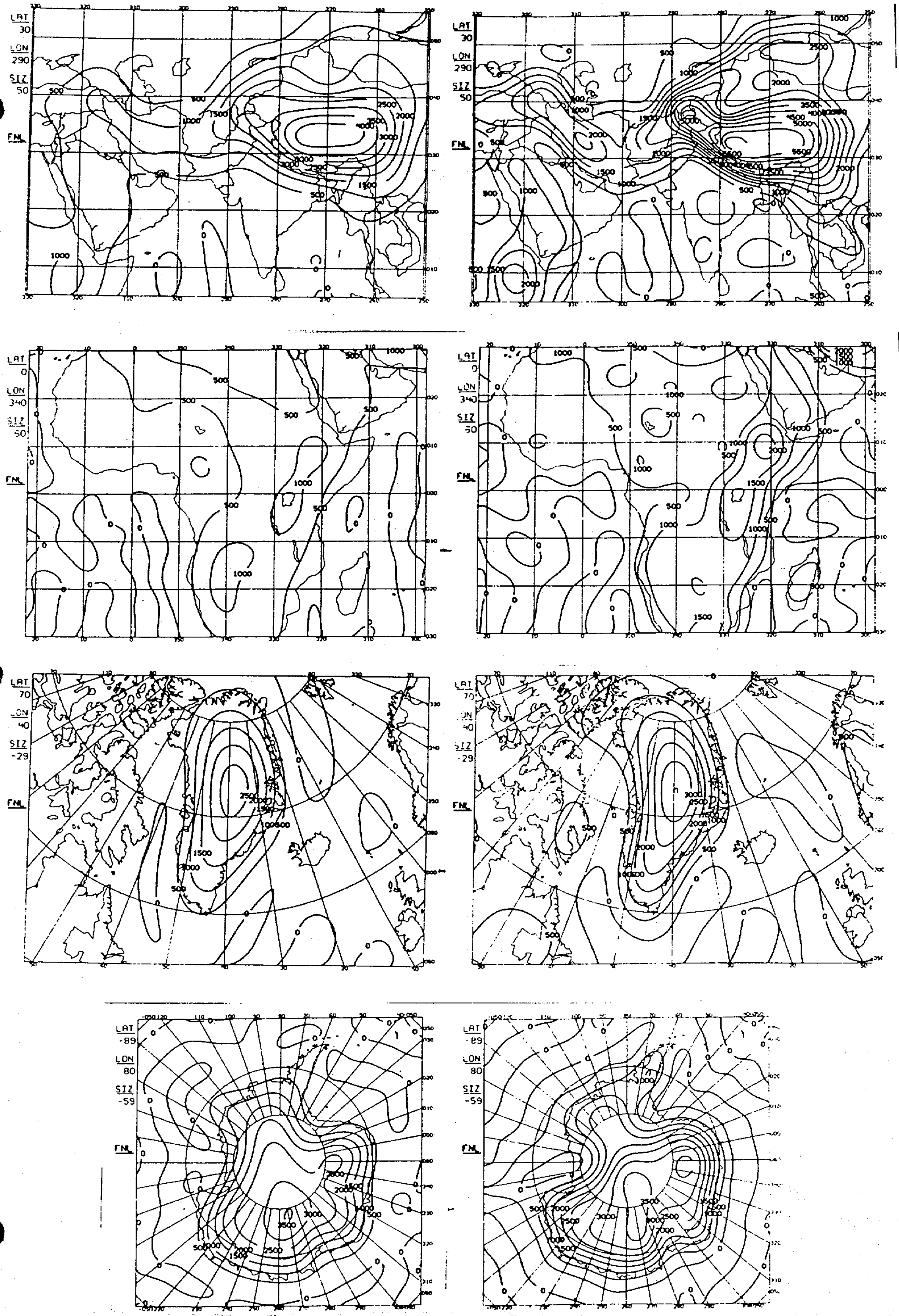

Figure 1. Continued

The virtual temperature correction consists of the removal of an approximation that has always been part of the NMC spectral models - the use of the virtual temperature (as derived hydrostatically from the initial geopotential field) in places in the model where the use of true temperature would be more exact. Two areas required changes; one involves the diabatic adjustments - (dry convection, moist convection, and large-scale precipitation) - the other, the initial calculation of the specific humidity field, given the virtual temperature and relative humidity fields. The specific humidity, q, is given by

$$q = r.h. \times q_s(T)$$

where $q_s(T)$ is the saturation specific humidity at the true temperature and r.h. is the relative humidity. Since T can't be recovered from the virtual temperature T_v without prior knowledge of q itself, it is necessary to iterate a few times to get an accurate initial q field. In the operational model, what is done is simply to substitute $q_s(T_v)$ for $q_s(T)$. The more accurate method produces a smaller initial q, especially near the surface in the tropics, where T_v-T may be on the order of a few degrees, and the accurate q several g/kg smaller than the approximate q. For example, if T_v = 30C and r.h. = 0.50, the uncorrected q estimate gives 13.4 g/kg at 1000 mb, while the corrected q turns out to be 11.8 g/kg. Initially, at least, the smaller q's should inhibit slightly the long-wave radiational warming; however, the error should tend to be self-correcting as the lower atmospheric q values enhance the surface-to-air q gradient and increase evaporation rates.

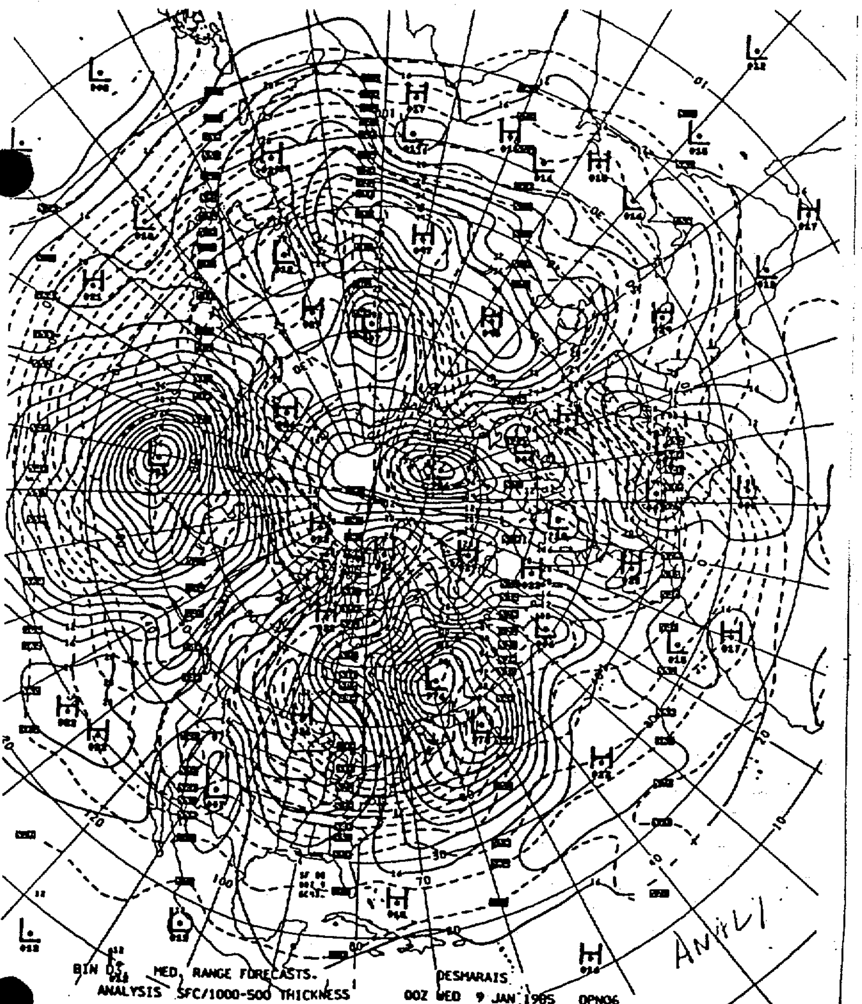

00Z Jan. 9, 1985

00Z Jan. 24, 1985

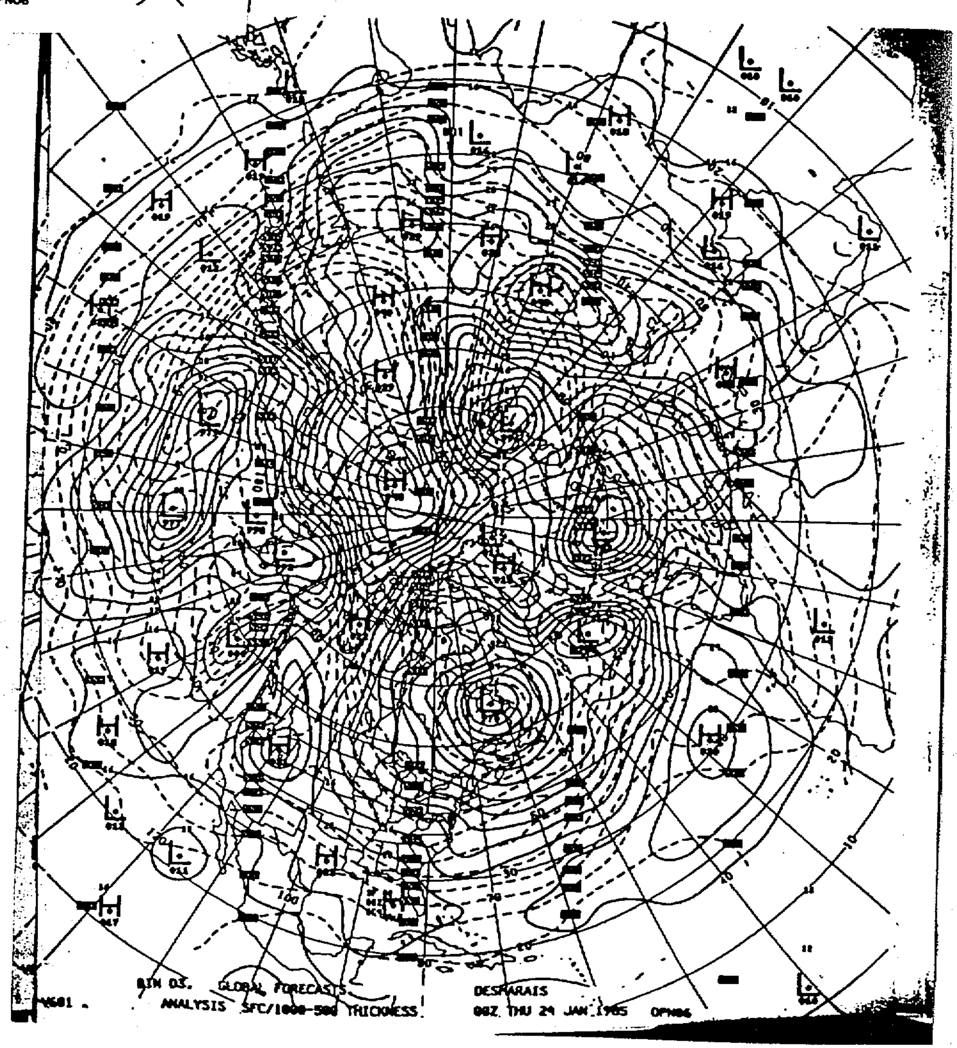

Figure 2. Initial Analyses

Case of Jan. 24

The combined effects of the virtual temperature correction and the silhouette mountains were tested on the January 24 run (initial analysis shown in Fig. 2), for which a series of Northern Hemisphere sea level pressure and 1000-500 mb thickness charts are shown below (Figures 3 and 4). The four charts compared in each figure are, reading clockwise from the upper left, (1) the new medium-range spectral with corrections described above (MR*); (2) the new medium-range spectral without the corrections (MR); (3) the analysis valid at the relevant time; and (4) the operational spectral model.

Conditions at 72 hours: At this point in the forecast, the MR and the MR* are very much alike as to the positions and general shapes of most systems. The only area of striking difference is around the high elevations of southern Asia, where the MR* has produced a 1002 mb low along latitude 30° that is completely absent in the MR and the operational. The isobars appear quite a bit noisier over land in the MR* than in the MR.

There is little difference in the forecasting of the two major low systems - one south of Greenland, the other near the Aleutians. Both the MR and the MR* are superior to the operational in their thermal and pressure fields for these systems.

120 hours: By this time, significant differences are apparent. While the operational came closest to forecasting the intensity of the 947 mb Newfoundland low, the MR* was the only one of the three to move it far enough to the east. All three models predicted a large east-west oriented system

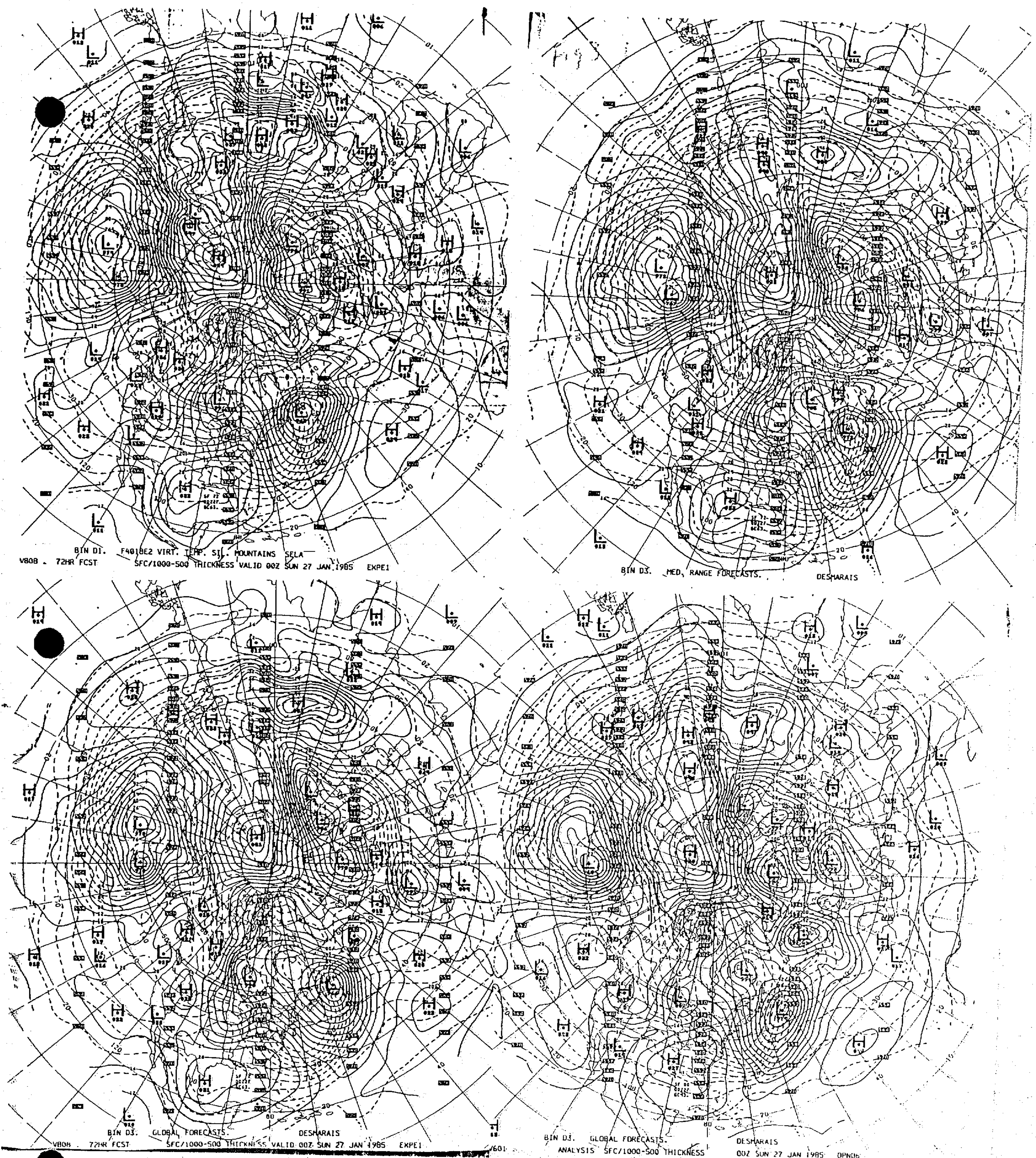

Figure 3. Surface isobars and 1000-500 mb thickness contours at 72 hours. Upper left: MR*; upper right: MR; lower left: operational; lower right: analysis. (Case of Jan. 24)

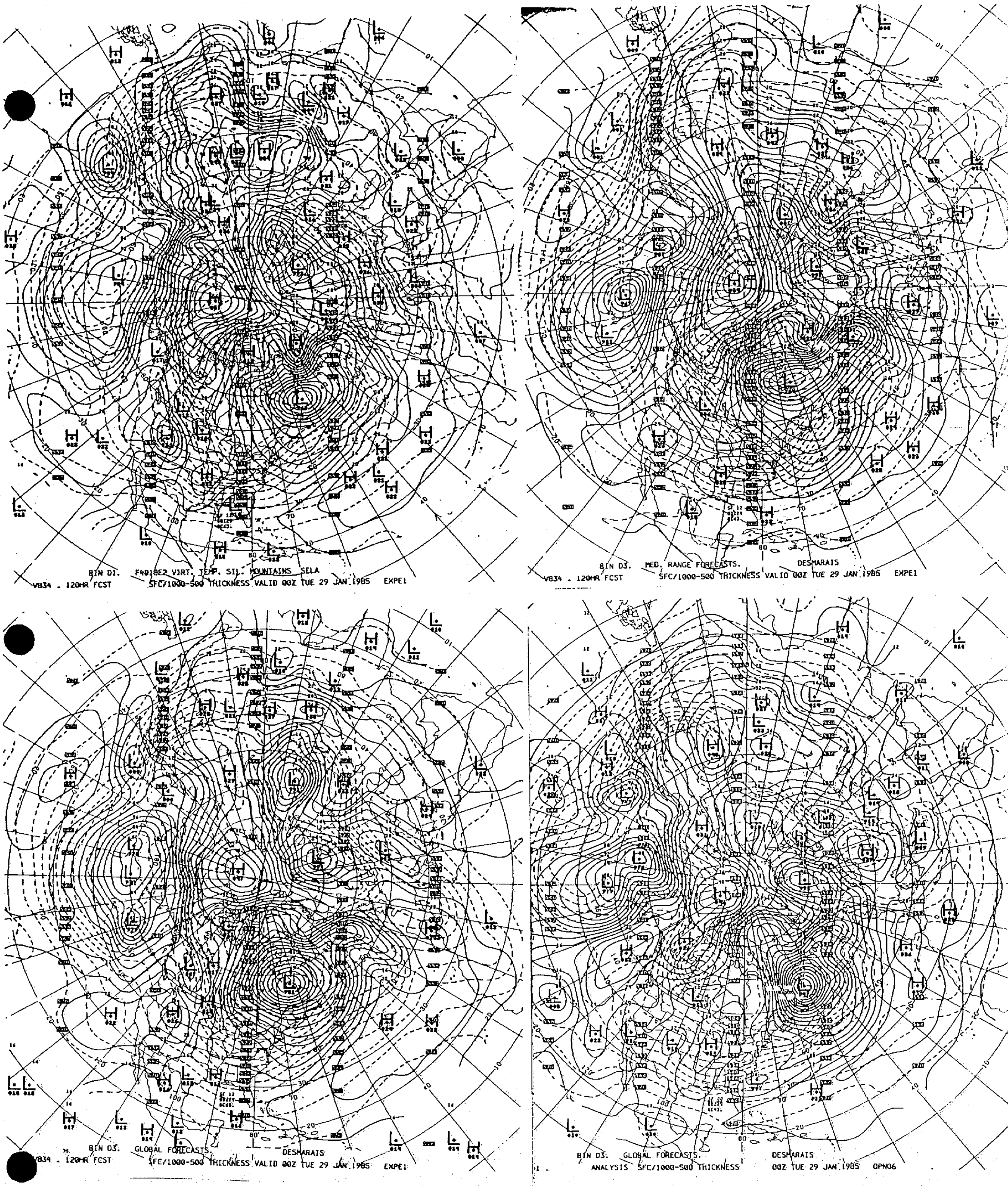

Figure 4. As in Fig. 3, but for 120 hours (case of Jan. 24)

in the North Pacific, but the MR* was too weak on its intensity. The MR* did extremely well, however, in creating three small wave cyclones - in Florida, off Japan, and in the eastern Mediterranean - that verified and that were missed for the most part by the two other forecasts. There is some indication that in undisturbed tropical areas the virtual temperature correction is causing the MR* to be a few decameters colder in thickness by 120 hours than the MR, which in turn is slightly colder than the analysis.

Case of Jan. 9:

The one case available in which there is a clean comparison involving only the change in mountains is the run initialized on January 9 at 00Z (Fig. 2). As it happens, interesting differences show up earlier in this case than in the January 24 case, in particular in three systems - a low initially in the Mediterranean, a wave perturbation in the east central Pacific, and the large anticyclone covering North America. The forecast maps for this case (Figs. 5 and 6) are arranged as in the January 24 case.

Conditions at 48 hours: During the first two days (Fig. 5), the MR deepens the Mediterranean low by 20 mb and moves it just north of the Black Sea, while the model with the silhouette mountains (MR*) deepens it only by 11 mb to 991 mb and creates a weak east-west oriented trough (which verified). The operational deepened the low by 29 mb, while the analysis shows a 3-mb weakening. The Pacific wave was observed to move rapidly northeastward to a position just southwest of Alaska at 973 mb, with a disorganized second wave showing up about 1000 km off the Washington coast. The MR seems to have lost the first wave, while both the operational and the MR* both did an excellent job on intensity as well as on position. The North American

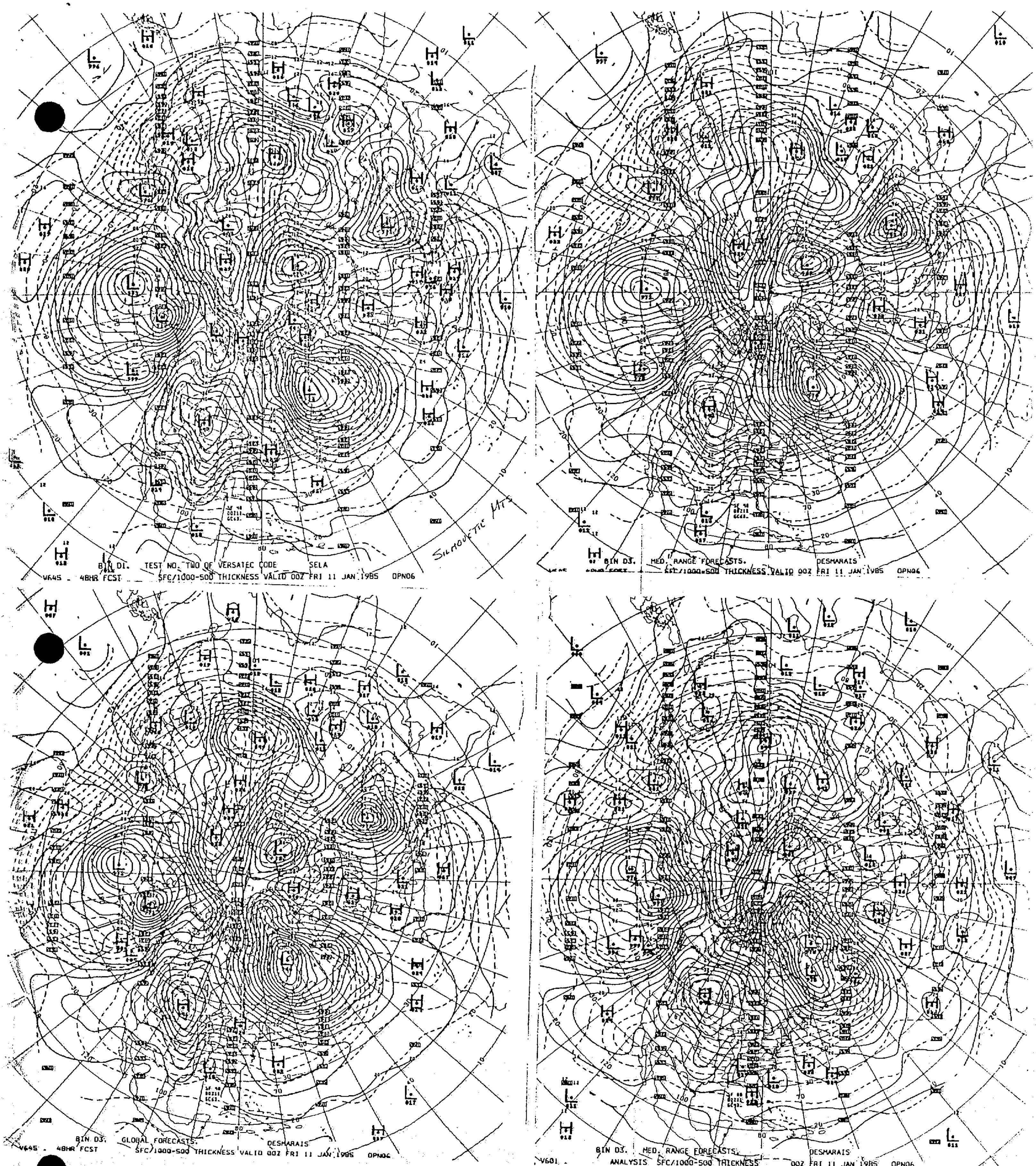

Figure 5. As in Fig. 3, but for 48 hours (case of Jan. 9)

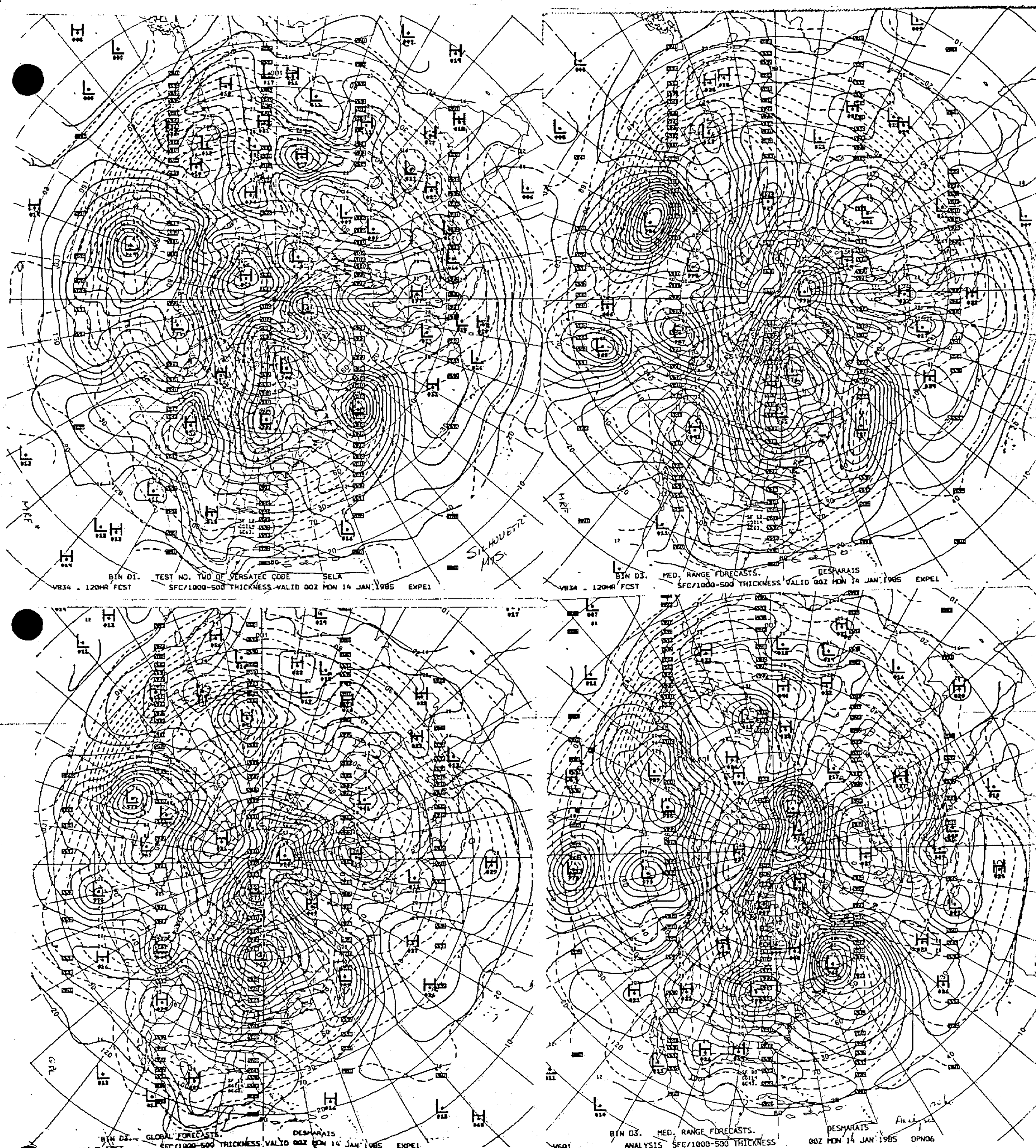

Figure 6. As in Fig. 3, but for 120 hours (case of Jan. 9)

anticyclone was handled best by the MR*, which showed the most realistic southward ridging through Texas and Nevada and troughing in New Mexico. The Alabama wave was handled equally well by the two forecasts.

120 hours: Over the next three days the U.S. anticyclone was observed to remain nearly stationary while a cyclone formed in the lee of the Canadian Rockies and occluded over Lake Superior on the arctic front (Fig. 6). The Alabama trough had moved northeastward and matured to a 968-mb low off Newfoundland, and a wave appeared in the Caribbean. A new wave formed in the central Pacific and was progressing eastward along latitude 30°, and a trough developed northeast of Japan. Both medium-range models picked up the Lake Superior system rasonably well, with the MR* doing a good job on the Caribbean wave. The MR* looked excellent on the Newfoundland system - far better in both intensity and shape than the other models. However, it missed the low-latitude Pacific wave almost entirely, having weakened it in the last 24 hours, while the other models strengthened it. Finally, the Japan trough was overdeveloped by all of the models, most notably by the MR.

Statistical Comparison

While no objective statistical comparisons are available for the two particular cases presented above, we do have available a set of Northern Hemisphere anomaly correlations at the 500 mb level for a sample of five-day forecasts taken from December and January before the correction and another set for late January and February forecasts after the corrections. The "after" forecasts showed a substantially higher average score (.739) than the "before" forecasts (.646), but it happened that there was also an improvement in the operational forecasts, which were .635 during the "after" sample, up from .601 during the "before" sample. For this reason, the best statistic to look at is the differences in score, (1) MR - operational vs. (2) MR* - operational. For a sample of 27 cases of each, the results as shown in Table 1 below were clearly in favor of the MR*, .104 vs. .045, with standard deviations of .080 and .075, respectively. The 't' statistic shows that the 95% confidence interval for these means is about .03, so the difference would be highly significant if we were dealing with independent events. Independence is certainly not the case here, because most of the test were made on consecutive days, with just a few days missing. However, the results are quite convincing if looked at non-parametrically, e.g., comparing the MR and the the MR* to the operational in terms of wins, losses, and ties. Here the figures for the MR are 15 wins, 9 losses, and 3 ties; the MR*, 24 wins, 1 loss, and 2 ties.

Table 1. Comparison of medium-range models versus operational before and after the virtual temperature and silhouette mountain changes. The bottom line is the 95% confidence interval for the sample mean, based on the t statistic.

	BEFORE CHANGE (N=27)			AFTER CHANGE (N=27)		
	Operational	MR	MR-Opnl	Operational	MR*	MR*-Opnl
mean	.601	.646	.045	.635	.739	.104
s.d.	.104	.101	.080	.079	.066	.075
95% C.I.	±.042	±.041	±.032	±.032	±.027	±.030

Conclusions:

On the basis of just the two cases for which the surface maps were analyzed, while both of the medium-range forecast are better than the operational, it is difficult to prove the superiority of the MR* over the MR. The differences that do emerge however are (1) a tendency for mature cyclones to be less intense in the MR* than in the MR and (2) for anticyclones over high terrain to be extra strong in the MR*, probably a result of sea-level pressure reduction problems. The 1000-500 mb thickness field of the MR* seems consistently a bit colder than that of the MR, judging from contour values in undisturbed tropical regions.

The 500-mb statistics for the 54 cases examined make a much better case for choosing of the MR* over the MR and also clearly establish the superiority of the medium-range spectral models over the operational model.

Reference

Mesinger, F., 1985: The sigma system problem. Preprint volume, Seventh Conference on Numerical Weather Prediction, Montreal. To be published.